

Title: A global analysis of subsidence, relative sea-level change and coastal flood exposure

Authors:

5 Robert J. Nicholls¹, Daniel Lincke², Jochen Hinkel^{2,3}, Sally Brown⁴, Athanasios T. Vafeidis⁵,
Benoit Meyssignac⁶, Susan E. Hanson⁷, Jan Merckens⁵, Jiayi Fang⁸

Affiliations:

¹ Tyndall Centre for Climate Change Research, University of East Anglia, Norwich, UK

10 ² Global Climate Forum e.V. (GCF), Berlin, Germany

³ Division of Resource Economics, Albrecht Daniel Thaer-Institute and Berlin

Workshop in Institutional Analysis of Social-Ecological Systems (WINS), Humboldt-

University, Berlin, Germany

⁴ Department of Life and Environmental Sciences, Faculty of Science and Technology,

15 Bournemouth University, UK

⁵ Kiel University, Department of Geography, Kiel, Germany

⁶ LEGOS, Université de Toulouse, CNES, CNRS, UPS, IRD, 31400 Toulouse, France.

⁷ School of Engineering, University of Southampton, Southampton, UK

⁸ School of Geographic Sciences, East China Normal University, Shanghai, 200241,

20 China

ORCID

Robert J. Nicholls 0000-0002-9715-1109

Daniel Lincke 0000-0003-4250-5077

25	Jochen Hinkel	0000-0001-7590-992X
	Sally Brown	0000-0003-1185-1962
	Athanasios T. Vafeidis	0000-0002-3906-5544
	Benoit Meyssignac	0000-0001-6325-9843
	Susan E. Hanson	0000-0002-2198-1595
30	Jan Merkens	0000-0003-0916-2906
	Jiayi Fang	0000-0002-0420-5615

Editors Summary:

35 Land subsidence/uplift influences the rate of sea-level rise. Most coastal populations live in subsiding areas and as a result experience average rates of relative sea-level rise three to four times faster than due to climate change alone. This indicates the need for policy to address subsidence.

40 Abstract:

Climate-induced sea-level rise and vertical land movements, including natural and human-induced subsidence in sedimentary coastal lowlands, combine to change relative sea levels around the world's coast. Although this affects local rates of sea-level rise, assessments of the coastal impacts of subsidence are lacking on a global scale. Here, we quantify global-mean
45 relative sea-level rise to be 2.5 mm/yr over the last two decades. However, as coastal inhabitants are preferentially located in subsiding locations, they experience an average relative sea-level rise up to four times faster at 7.8 to 9.9 mm/yr. These results indicate that the impacts and adaptation needs are much higher than reported global sea-level rise measurements suggest. In particular, human-induced subsidence in and surrounding coastal cities can be rapidly reduced
50 with appropriate policy for groundwater utilization and drainage. Such policy would offer substantial and rapid benefits to reduce growth of coastal flood exposure due to relative sea-level rise.

Main Text:

55 It is widely recognised that climate-induced sea-level rise (SLR) is raising water levels around
the world's coast¹⁻³ and that this will lead to an increase in flood risk and other impacts unless
there is corresponding adaptation⁴. Against this background, a large literature has assessed the
magnitude of SLR, and its impacts and adaptation needs at global scales². Indeed, this literature
is essential for setting and evaluating mitigation targets, strategic adaptation, and designing
60 financial arrangements for funding adaptation and compensation for loss and damage. Over time,
this literature has progressed from focusing on climate-induced regional SLR to also including
geological sources of local relative sea-level change such as glacial-isostatic adjustment (GIA) in
order to serve local adaptation needs, for which the source of relative SLR is irrelevant. To our
knowledge, however, no global study has quantitatively considered the contribution of
65 subsidence to global SLR risk. This may constitute a serious limitation in global exposure
estimates as human-induced subsidence in particular can lead to rates of local SLR that are much
higher than current rates of climate-induced SLR. Furthermore, these high rates occur
specifically in densely populated areas such as cities and deltas. This could have a large effect on
people's experience of relative sea-level rise, but so far the size of this effect has not been
70 studied at global scales.

Important geological processes that are contributing to relative sea-level change include
tectonics, glacial-isostatic adjustment (GIA) and subsidence in geologically recent sedimentary
deposits such as deltas, which can be significantly enhanced by human agency especially
75 groundwater withdrawal⁵⁻¹⁰. As global models are available (e.g., Peltier et al¹¹) and it is a long-
term stable process causing either uplift or subsidence depending on location, GIA is often

considered in global analysis of relative sea level and impacts. Other sources of land elevation change are not regularly included, being implicitly seen as a local problem.

80 Natural subsidence, mainly due to the compaction of young sediments in deltas, is widespread and significant¹². However, the most rapid rates of subsidence are human-induced. These are caused by accelerated compaction primarily due to withdrawal of underground fluids including groundwater, oil and gas, as well as drainage of organic soils^{8,12}. As Ericson et al¹³, Syvitski et al¹⁴ and Tessler et al¹⁵ among others have demonstrated, these processes are marked in many of
85 the world's deltas and are often compounded by both local flood defences within the delta and upstream dams, which collectively reduce the sediment supply that maintains these sedimentary landforms. Sand extraction and mining can exacerbate this loss of sediment supply.

Cumulatively, human effects on subsidence are at their largest in some coastal cities located on deltas and alluvial plains: a net subsidence of more than 4 m has occurred during the 20th
90 century in parts of Tokyo, and 2 to 3 m in Shanghai, Bangkok, Jakarta and New Orleans¹⁶⁻¹⁹. Many deltas and subsiding cities are in Asia and the World Bank²⁰ recognised that subsidence could be as significant as climate-induced SLR in parts of coastal Asia over the 21st century.

To analyse the relative importance of subsidence on relative SLR, we consider data for four
95 components of relative sea-level change: (1) climate-induced sea-level change^{21,22}; (2) glacial-isostatic adjustment (GIA)¹¹; (3) recent estimates of total deltaic subsidence, including natural and human-induced changes; and (4) recent estimates of human-induced subsidence in coastal cities on deltas and alluvial plains (which operate at a sub-delta scale and hence is additional to the subsidence due to component 3). In addition to the individual components, we also consider

100 the combined effect of all these components, which is the local relative SLR. To compute global
relative SLR, we weight local relative SLR values by the length of coast and thus obtain an
estimate of the average relative SLR per kilometre of coast. Given that the distribution of coastal
population and hence SLR risks and adaptation needs are not uniform, we also estimate the
global relative SLR weighted by coastal population, giving an estimate of the average relative
105 SLR per coastal resident. We then consider the relative role of subsidence in enhancing coastal
flood risk to 2050 compared to other changes, assuming current estimates of subsidence
continue. For this, we focus on the coastal flood plain population (i.e., exposure) as a metric as it
is independent of adaptation. All components, data and methods are defined and described in
more detail in the Methods.

110
Considering weighting by coastal length, the analysis shows that contemporary global-mean
coastal relative SLR, including climate and geological components, averages 2.5 mm/yr over the
last two decades with climate-induced SLR being the dominant component (Fig. 1; Table 1).
This is less than the climate-induced change component alone as GIA causes a net average fall in
115 relative sea level around the world's coasts. Globally, the combined effect of subsidence
components in deltas and coastal cities is almost negligible and cannot be distinguished in the
cumulative distribution curve (Extended Data Fig. 1). This reflects that, based on the data
analysed, only 6.5 percent and 0.8 percent of the world's coast comprises subsiding deltas and
subsiding cities respectively.

120

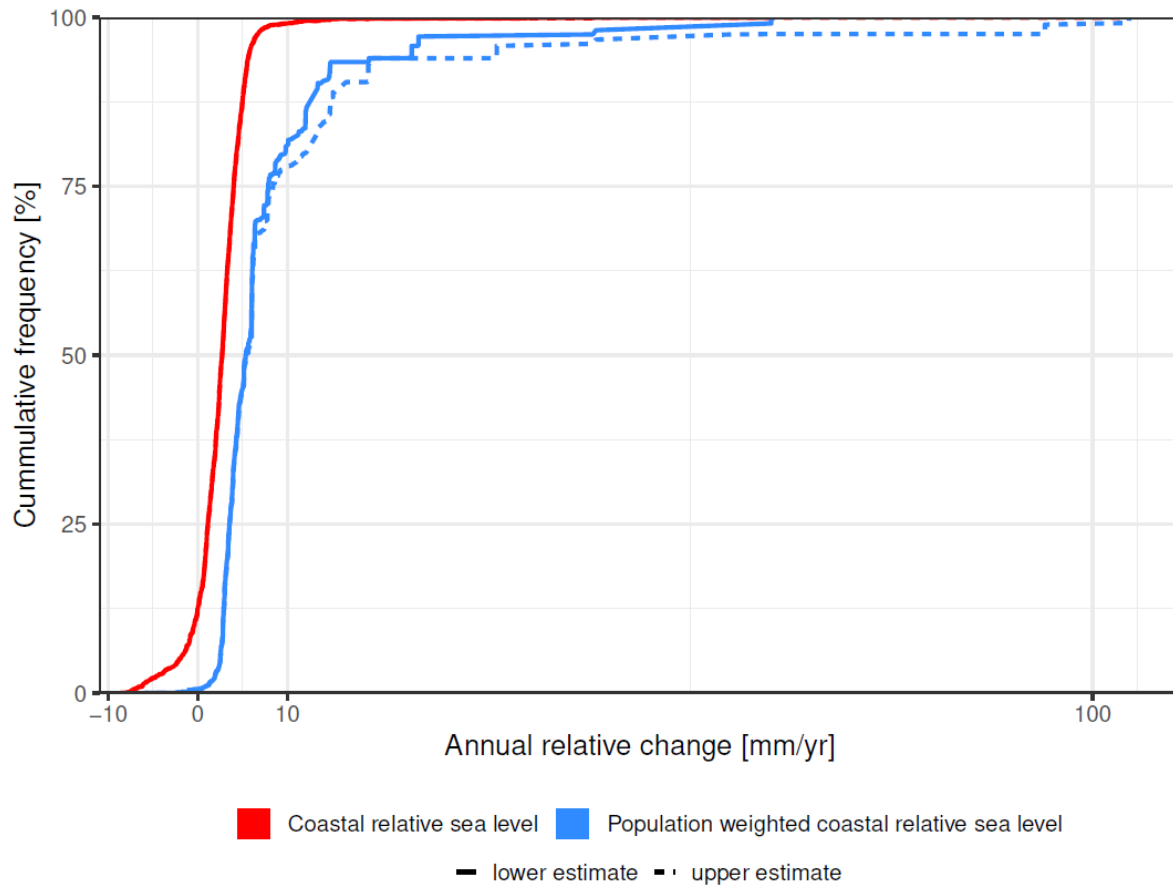


Fig 1: Cumulative distribution of contemporary (last two decades) length-weighted and population-weighted coastal relative sea-level rise, respectively. This includes lower and upper estimates to express uncertainty, although for length weighting the difference is too small to be distinguished.

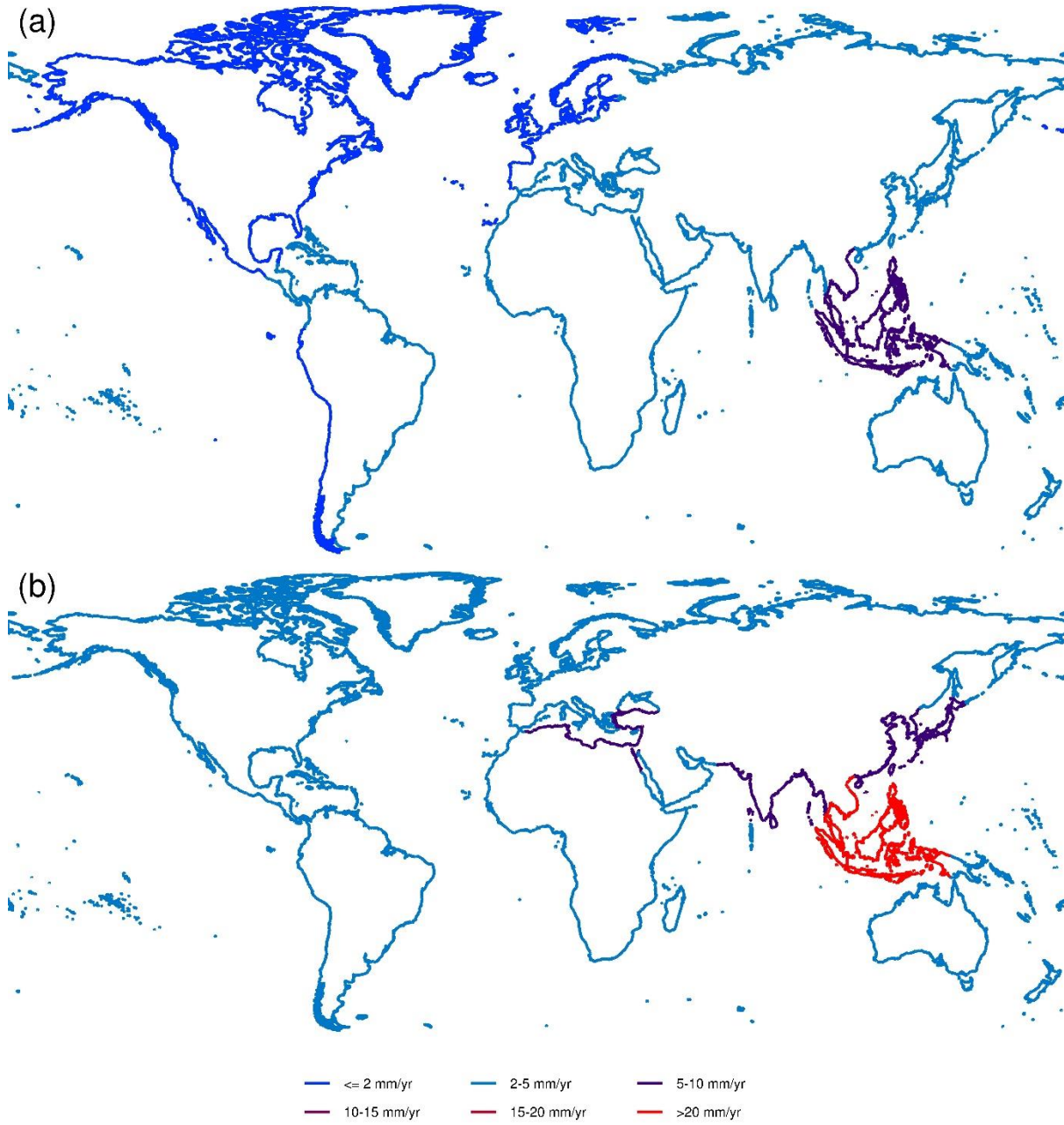
Table 1: Contribution of the climate and geological components to relative sea-level change for length-weighted and population-weighted cases respectively. Average values are reported, except for cities and the global-mean sum where a low/high range is used to express the uncertainty in subsidence (see Supplementary Table 2).

Relative SLR component	Contribution to relative sea-level change			
	Length-weighted		Population-weighted	
	mm/yr	%	mm/yr	%
Climate-induced SLR (1993 to 2015)	3.2	122	3.8	39 to 49
Glacial Isostatic Adjustment	-0.8	-32	-0.3	-3
Delta Subsidence	0.1	4	1.6	16 to 21
City Subsidence	0.1	3	2.7 to 4.8	35 to 49
Global-mean sum	2.6		7.8 to 9.9	

In contrast, weighting by coastal population shows that coastal inhabitants on average experienced much higher relative SLR, reflecting the heterogeneous distribution of coastal population (Fig. 1, Table 1). The median relative SLR per person is about 5 mm/yr, while the mean is up to four times higher at 7.8 to 9.9 mm/yr over the last two decades. This global enhancement of average sea-level rise per person mainly reflects that coastal residents are concentrated in subsiding areas including deltas, and especially in subsiding coastal cities, which gives a high-end tail to the distribution (Fig. 1; Extended Data Fig. 1). Effectively, delta and city subsidence and population density are not independent - higher population densities lead to human actions that promote subsidence and loss of elevation. Furthermore, deltas have fertile soils and hence have historically been hotspots for human management and development¹⁴. Hence, the relative sea-level change components linked to human activities tend to increase with population density around the world's coasts (Extended Data Fig 2). We estimate that 51 to 70 percent of the total global average relative SLR experienced by people is due to delta and city subsidence (Table 1). In contrast, the global effect of GIA is almost negligible when considering population weighting (Extended Data Fig. 1).

Globally, average sea-level changes over the last two decades are distributed unevenly across coastal length and coastal population (Fig. 1). About 12.5 percent of the world's coast by length is experiencing relative sea-level fall, this being attributed to uplift caused by GIA. However, these areas only have 2.7 million inhabitants (less than one percent of global coastal population). Conversely, only about 0.7-0.8 percent of the world's coast by length is experiencing a SLR above 10 mm/yr (the range covers uncertainty in city subsidence). However, these coasts contain large subsiding cities such as Jakarta and 147 to 171 million inhabitants (19.1-22.3 percent of the global coastal population).

Average coastal population-weighted relative sea-level rise is also often higher at the regional level than coastal-length weighted relative sea-level rise estimates (Fig 2): 11 of 23 world regions show more than 50 percent increases in population-weighted relative sea-level rise when compared to coastal length-weighted relative sea-level rise (Supplementary Table 4). Seven regions have an increase of more than 100 percent (the Baltic Sea Coast, North and West Europe, North America Atlantic Coast, North America Pacific Coast, South America Pacific Coast, Southern Mediterranean and South-East Asia), reflecting regions where coastal residents are strongly concentrated in areas where relative sea-level rise is higher. In absolute terms, the effect in South, South-east and East Asia is noteworthy (Supplementary Table 4), as these regions collectively contain 71% of the global coastal population below 10-m elevation (546 million out of 768 million people globally in 2015) and 75% of the global coastal floodplain population (185 million out of 249 million people globally in 2015).



160

Fig 2: Average relative sea-level rise for 23 coastal world regions. (a) Length-weighted and (b) population-weighted. (see Supplementary Table 3 for region definitions).

165 Finally, we assess the contributions of climate-induced SLR, GIA, delta subsidence and city
subsidence to the evolution of the global population living in the coastal flood plain from 2015 to
2050 (Fig. 3). This assumes that the observed subsidence in deltas and cities continues to 2050,
representing a plausible scenario of future subsidence. In 2015, this flood plain population is
approximately 235 million people. Assuming no subsidence and no climate-induced SLR, this
population rises to about 280 million people by 2050 due to socio-economic development alone
(here SSP2)²³. Adding the GIA component, reduces this number to 270 million, while adding the
170 delta subsidence component increases it back to about 280 million people. Adding the
uncontrolled city subsidence component further increases the flood plain population to about 305
to 320 million people (a net increase of 25 to 40 million people summing across the GIA, delta
and city subsidence components). Additionally considering climate-induced SLR, the exposed
population increases to 330 to 350 million by 2050 (a net increase of 25 to 30 million people due
175 to climate change) (Fig. 3(d)). The effects of subsidence and climate-induced SLR on exposed
population numbers can therefore be seen as being comparable in magnitude over the next 30
years. Under other SSPs, the results are similar (see Extended Data Fig, 3).

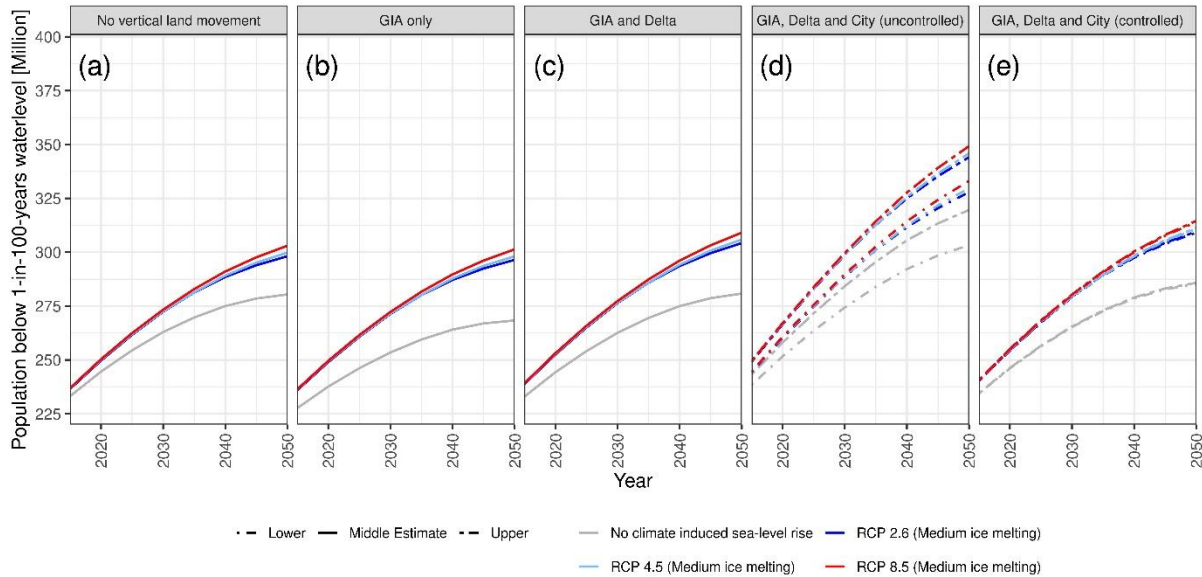


Fig 3: Global population in the coastal flood plain from 2015 to 2050. This considers sea-level rise scenarios under RCP2.6, RCP4.5 and RCP8.5 emissions, as well as no climate-induced sea-level rise as a reference, and assumes the SSP2 socio-economic scenario. Subsidence/GIA assumptions as indicated. (a) No vertical land movement. (b) GIA only. (c) GIA and delta subsidence. (d) GIA, delta and uncontrolled city subsidence. (e) GIA, delta and city subsidence controlled to 5 mm/yr. The uncertainty bands reflect uncertainty in rates of city subsidence (see Fig. 1). Simulations start in 1995, while the flood plain is defined based on the 100-year event.

180 These findings have important implications for coastal management, climate action and sustainability goals. For climate mitigation, they mean that contemporary and future global SLR risks and adaptation needs are much higher than previously assessed. For adaptation, this means that reducing human-induced subsidence constitutes a globally significant coastal adaptation option. While from a conceptual point of view it can be debated if managing subsidence

185 constitutes adaptation, from a practical point of view this has a higher potential for reducing

coastal exposure than climate mitigation over the next 30 years. For example, if we reduce coastal city subsidence to 5 mm/yr, population exposure could be reduced by about 20 to 35 million people or 6 to 10 percent by 2050 compared with unreduced city subsidence (Fig. 3e compared to Fig. 3d), whereas under ambitious climate mitigation (i.e., from RCP8.5 to RCP2.6), population exposure would be reduced by about 5 million people or 1.5 percent over the same timeframe. Climate mitigation would lead to much larger benefits after 2050^{2,24} (not assessed here), and these two policies can and should be complementary. Reducing city subsidence to 5 mm/yr or less is feasible as demonstrated in the Netherlands and many Asian cities (e.g., Tokyo, Osaka, Shanghai), where it involves managing groundwater withdrawal and maintaining high water tables. However, these policies generally reduce rather than stop all subsidence^{9,17} and there are wider implications and risks associated with rising water tables for cities. Therefore, while some subsidence control may be feasible, other SLR adaptation approaches will still be necessary and compatible with adapting to climate change^{2,18}. Controlled flooding and sedimentation could be an innovative response to loss of elevation in deltas, especially in agricultural areas. This would involve a major shift in thinking in delta management to controlling rather than eliminating flooding, and recognising sediment and sedimentation as a resource^{14,25,26}.

The influence of subsidence on relative SLR has grown through the 20th century alongside expanding coastal populations in susceptible areas – notably in deltas and especially in large and expanding cities on those deltas. The results discussed here indicate this will certainly continue and maybe even grow in magnitude and extent with increasing coastal urbanisation in susceptible settings. Improved measurements of natural and human-induced subsidence

processes are emerging and analysed systematically, as shown here, this will allow fuller
210 appreciation of the potential consequences of relative SLR at regional to global scales and
appropriate responses developed²⁷⁻²⁹.

In conclusion, this analysis shows that, due to its coincidence with major population centres,
subsidence has global social and economic implications. Its influence on exposure to coastal
215 flooding is comparable to, if not greater than, climate-induced sea-level rise over the next few
decades and will remain significant thereafter. As such, subsidence should be better recognized
in regional and global assessments of relative sea-level rise impacts, and not simply restricted to
local assessments. This, in turn, would improve the evidential basis for adaptation, disaster risk
reduction, and development strategies in coastal areas.

220 **References:**

- 1 Nerem, R. S. *et al.* Climate-change–driven accelerated sea-level rise detected in the
altimeter era. *Proceedings of the National Academy of Sciences* **115**, 2022,
<https://doi.org/10.1073/pnas.1717312115> (2018).
- 225 2 Oppenheimer, M. *et al.* in *IPCC Special Report on the Ocean and Cryosphere in a
Changing Climate* (eds H O Pörtner *et al.*) Ch. 4 Sea level rise and implications for low
lying islands, coasts and communities, (Intergovernmental Panel on Climate Change
(IPCC), 2019)
- 3 Church, J. A. *et al.* in *Climate Change 2013: The Physical Science Basis. Contribution of
Working Group I to the Fifth Assessment Report of the Intergovernmental Panel on
230 Climate Change* (eds T F Stocker *et al.*) Ch. 13 Sea level change, 1137-1216 (Cambridge
University Press, 2013)
- 4 Wong, P. P. *et al.* in *Climate Change 2014: Impacts, Adaptation, and Vulnerability, Pt A:
Global and Sectoral Aspects: Working Group II Contribution to the Fifth Assessment
Report of the Intergovernmental Panel on Climate Change* (eds C. B. Field *et al.*) Ch. 5
235 Coastal systems and low-lying areas, 361-409 (2014)
- 5 Emery, K. O. & Aubrey, D. G. *Sea Levels, Land Levels, and Tide Gauges*. (Springer-
Verlag, 1991).
- 6 Rovere, A., Stocchi, P. & Vacchi, M. Eustatic and relative sea level changes. *Current
Climate Change Reports* **2**, 221-231, <https://doi.org/10.1007/s40641-016-0045-7> (2016).

- 240 7 Lickley, M. J., Hay, C. C., Tamisiea, M. E. & Mitrovica, J. X. Bias in estimates of global
mean sea level change inferred from satellite altimetry. *Journal of Climate* **31**, 5263-
5271, <https://doi.org/10.1175/JCLI-D-18-0024.1> (2018).
- 8 Milliman, J. & Haq, B. U.(eds) *Sea-Level Rise and Coastal Subsidence: Causes,
Consequences, and Strategies*. (Springer, 1996).
- 245 9 Erkens, G., Bucx, T., Dam, R., de Lange, G. & Lambert, J. Sinking coastal cities. *Proc.
IAHS* **372**, 189-198, <https://doi.org/10.5194/piahs-372-189-2015> (2015).
- 10 Frederikse, T., Riva, R. E. M. & King, M. A. Ocean bottom deformation due to present-
day mass redistribution and its impact on sea level observations. *Geophysical Research
Letters* **44**, 12,306-312,314, <https://doi.org/10.1002/2017GL075419> (2017).
- 250 11 Peltier, W. R., Argus, D. F. & Drummond, R. Space geodesy constrains ice age terminal
deglaciation: The global ICE-6G_C (VM5a) model. *Journal of Geophysical Research:
Solid Earth* **120**, 450-487, <https://doi.org/10.1002/2014JB011176> (2015).
- 12 Syvitski, J. P. M. Deltas at risk. *Sustainability Science* **3**, 23-32,
<https://doi.org/10.1007/s11625-008-0043-3> (2008).
- 255 13 Ericson, J. P., Vörösmarty, C. J., Dingman, S. L., Ward, L. G. & Meybeck, M. Effective
sea-level rise and deltas: Causes of change and human dimension implications. *Global
and Planetary Change* **50**, 63-82, <https://doi.org/10.1016/j.gloplacha.2005.07.004>
(2006).
- 14 Syvitski, J. P. M. *et al.* Sinking deltas due to human activities. *Nature Geoscience* **2**, 681-
686, <https://doi.org/10.1038/ngeo629> (2009).
- 260 15 Tessler, Z. D., Vörösmarty, C. J., Overeem, I. & Syvitski, J. P. M. A model of water and
sediment balance as determinants of relative sea level rise in contemporary and future
deltas. *Geomorphology* **305**, 209-220, <https://doi.org/10.1016/j.geomorph.2017.09.040>
(2018).
- 265 16 Nicholls, R. J. Coastal megacities and climate change. *GeoJournal* **37**, 369-379,
<https://doi.org/10.1007/BF00814018> (1995).
- 17 Kaneko, S. & Toyota, T. in *Groundwater and Subsurface Environments: Human Impacts
in Asian Coastal Cities* (ed Makoto Taniguchi) Ch. Long-term urbanization and land
subsidence in Asian megacities: An indicators system approach, 249-270 (Springer
270 Japan, 2011) https://doi.org/10.1007/978-4-431-53904-9_13
- 18 Esteban, M. *et al.* Adaptation to sea level rise: Learning from present examples of land
subsidence. *Ocean & Coastal Management* **189**, 104852,
<https://doi.org/10.1016/j.ocecoaman.2019.104852> (2020).
- 275 19 Burkett, V. B., Zilkowski, D. B. & Hart, D. A. in *Proceedings of USGS Aquifer
Mechanics and Subsidence Interest Group conference, Galveston, TX, USA 27–29
November 2001. USGS water resources division open-file report series 03-308* (eds K R
Prince & D. L. Galloway) Ch. Sea level rise and subsidence: implications for flooding in
New Orleans, Louisiana, 63-70 (US Geological Survey, 2003)
- 20 World Bank. Climate risks and adaptation in Asian coastal megacities: A synthesis
report. 97pp (World Bank, Washington DC, USA, 2010)
- 280 21 Ablain, M. *et al.* Improved sea level record over the satellite altimetry era (1993–2010)
from the Climate Change Initiative project. *Ocean Science* **11**, 67-82,
<https://doi.org/10.5194/os-11-67-2015> (2015).

- 285 22 Legeais, J. F. *et al.* An improved and homogeneous altimeter sea level record from the
ESA Climate Change Initiative. *Earth Systems Scientific Data* **10**, 281-301,
<https://doi.org/10.5194/essd-10-281-2018> (2018).
- 23 Krieglner, E. *et al.* A new scenario framework for climate change research: the concept of
shared climate policy assumptions. *Climatic Change* **122**, 401-414,
<https://doi.org/10.1007/s10584-013-0971-5> (2014).
- 290 24 Nicholls, R. J. *et al.* Stabilization of global temperature at 1.5°C and 2.0°C:
implications for coastal areas. *Philosophical Transactions of the Royal Society A:
Mathematical, Physical and Engineering Sciences* **376**, 20160448,
<https://doi.org/10.1098/rsta.2016.0448> (2018).
- 295 25 Day, J. W. *et al.* Restoration of the Mississippi Delta: Lessons from Hurricanes Katrina
and Rita. *Science* **315**, 1679, <https://doi.org/10.1126/science.1137030> (2007).
- 26 Darby, S. E., Appearan Addo, K., Hazra, S., Rahman, M. M. & Nicholls, R. J. in *Deltas
in the Anthropocene* (eds Robert J. Nicholls, W. Neil Adger, Craig W. Hutton, & Susan
E. Hanson) Ch. 5 Fluvial sediment supply and relative sea-level rise, 103-126 (Springer
International Publishing, 2020) https://doi.org/10.1007/978-3-030-23517-8_5
- 300 27 Nicholls, R. J. *et al.* Sea-level scenarios for evaluating coastal impacts. *WIREs Climate
Change* **5**, 129-150, <https://doi.org/10.1002/wcc.253> (2014).
- 28 Erkens, G. & Sutanudjaja, E. H. Towards a global land subsidence map. *Proc. IAHS* **372**,
83-87, <https://doi.org/10.5194/piahs-372-83-2015> (2015).
- 305 29 Higgins, S. A. Review: Advances in delta-subsidence research using satellite methods.
Hydrogeology Journal **24**, 587-600, <https://doi.org/10.1007/s10040-015-1330-6> (2016).

Methods:

The analysis uses the framework of the Dynamic Interactive Vulnerability Assessment (DIVA)
310 model which has been applied to problems such as coastal erosion³⁰, coastal flooding³¹ and
coastal wetland change³², among others. The underlying structure is a dataset of coastal areas and
floodplains based on 12,148 coastal segments which divide the world's coast (excluding
Antarctica) into lengths of similar coastal characteristics³³. The segments are variable in length
with average of 70 km. All data such as sea-level rise (SLR), socio-economic development,
315 extreme water levels, subsidence rates, etc., is associated with the appropriate segment.

To analyse the global effects of subsidence on relative sea-level rise we combine data on four
components of relative sea-level change:

1. Satellite observations of sea-level change from 1993 to 2015;
2. Glacial-isostatic adjustment (GIA), derived from the model of Peltier et al¹¹;
- 320 3. Delta subsidence, which includes natural and anthropogenic subsidence in 117 deltas worldwide, building on the earlier work of Ericson et al¹³;
4. City subsidence, which captures the additional subsidence beyond delta subsidence that coastal cities in deltaic and alluvial plains experience. We thereby consider susceptible coastal cities with populations exceeding one million people in 2005 that are prone to
325 subsidence (following Nicholls et al³⁴).

These four components are independent and hence can simply be summed for each segment.

We exclude uplift and subsidence due to other processes such as tectonics⁶ as there are no consistent global datasets available. Most analysis of these processes are local or regional (e.g., National Research Council³⁵) and obtaining the data required to create relative sea-level rise
330 scenarios at the global scale is problematic²⁷. The few studies that systematically analyse data on vertical land movements globally using measurements at tide gauges^{36,37} find that GIA (already included in the analysis) explains a large part of the observed trends.

The major limitation in the analysis is that subsiding cities with less than one million are
335 excluded, again reflecting a lack of consistent data at the global scale. This means that our estimates of the effect of city subsidence on relative SLR are minimum estimates.

For assessing the effects of future climate-induced SLR we use the same scenarios as Hinkel et al³¹ For delta and city subsidence from 2015 to 2050, we assume that the observed rates of
340 subsidence continue at the same rate. It is recognised that these rates may be subject to

significant change, especially those due to human influence (e.g., Phien-wej et al³⁸). Hence, they should be considered as indicative scenarios rather than projections. The purpose of the analysis is to estimate the relative magnitudes of these processes rather than create projections.

345 For present and future population we use the scenarios of Merkens et al³⁹.

Data:

The following datasets are used in this analysis.

Sea-level change

350 For the sea-level change observations, we use the satellite altimetry product from the European Space Agency (ESA) Climate Change Initiative sea level (CCI_SL) project. We use this product because the data is computed with consistent geophysical corrections throughout the whole records and is thus specifically tailored for trend estimates^{21,22}. The product is a 2-D gridded sea surface height of delayed time anomalies described and validated in Legeais et al²². The product
355 is freely available on <http://www.esa-sealevel-cci.org/products>. We analysed the data over the period 1993 to 2015. The dataset is provided at monthly intervals on a $\frac{1}{4}^\circ$ regular grid as anomalies computed with reference to the 1993-2012 period. Sea-level anomalies for the study sites were extracted from the global dataset. At high latitude ($>82^\circ$), satellite altimetry data is not available (because of the inclination of the satellites). Close to the coast, data is available
360 until 15km from the coast. However, at 15 km from the coast some significant errors can arise in geophysical corrections applied to the sea level estimate. These errors arise from land contamination in the satellite radiometer measurement which is used for the wet-tropospheric

correction, or in the radar measurement which is used to estimate the altimetry range or in geophysical models such as tide models (because of inaccurate bathymetry for example). To
365 remove this potential spurious data we discarded all data at less than 25 km from the coast. To ensure that all spurious data was removed we checked that the difference between the data close to the coast and adjacent data offshore was within the typical sea level variability range (following The Climate Change Initiative Coastal Sea Level Team⁴⁰). For the trend estimate, we used a least square fit that estimate at the same time the annual cycle, the semi-annual cycle and
370 the trend. The uncertainty in the trend is estimated with an error budget approach and is below 3 mm/yr (at the 90% CL level²¹). Note that there is some difference between the coastal sea level trend and the sea level trend 25 km offshore. But this difference does not exceed 1.5 mm/yr (1 sigma value) over the satellite altimetry period (as shown by the difference between satellite altimetry and tide gauge records corrected for vertical land motion, see Wöppelmann and
375 Marcos⁴¹, or by the analysis from The Climate Change Initiative Coastal Sea Level Team⁴⁰).

Glacial Isostatic Adjustment (GIA)

Local sea-level change due to glacial isostatic adjustment caused by ice loading and unloading are taken from the ICE-6G_C (VM5a) model¹¹. Local land movement as response to
380 deglaciation and combined with global topography and bathymetry to compute local sea-level change on a 0.2°x0.2° grid. This gridded dataset is projected to the DIVA coastal segments by assigning the average sea-level change value over all intersected grid cells to each segment.

Delta subsidence

385 Delta subsidence is estimated for 117 deltas, comprising the world's most significant deltas. For
each delta a single indicative average value is assumed, except where stated otherwise, covering
a similar time period to the sea-level measurements. For 40 of the more populated deltas, data is
based on that developed by Ericson et al¹³, with a few corrections. These include the Ganges-
Brahmaputra delta where the value is taken from Brown and Nicholls⁴², the Mekong delta from
390 Erban et al⁴³ and Minderhoud et al⁴⁴, the North Italian Plain from Tos et al⁴⁵ and the Pearl River
delta from Wang et al⁴⁶. For the other 77 deltas, where there is little or no data, a minimum value
of subsidence is assumed in all cases at 1 mm/yr, following the estimates of Meckel et al⁴⁷. The
delta extent is linked to the DIVA segments. Supplementary Table 1 summarises the deltas
considered and subsidence values used.

395

Coastal city subsidence

The set of 136 coastal cities with more than one million people in 2005 as identified by Nicholls
et al³⁴ and Hallegatte et al⁴⁸ are considered in this analysis, with two additional coastal cities
within Indonesia which exceed the population threshold and are known to be subsiding:
400 Semarang and Medan⁴⁹. These large cities are considered in the analysis as they include the
largest urban populations and the largest observed subsidence is reported in some of them as
summarised in Supplementary Table 2. It is found that of these 138 cities, 36 cities are situated
wholly or partly on deltaic/alluvial deposits which may subside due to subsurface fluid
withdrawal and/or drainage. In each case, the additional subsidence beyond that captured in the
405 delta subsidence estimates (Supplementary Table 1) is estimated based on a survey of the
available literature or expert judgement if required. Given the wide range of values of subsidence

reported, a low and a high estimate of average subsidence are made to represent the uncertainty. These are applied as indicative average estimates across the subsiding area in each city. These estimates of subsidence covering a similar time period to the sea-level measurements. The extent of subsidence in each city is defined by the extent of Holocene deposits, which in turn is linked to the DIVA segments (i.e., subsidence is not applied to the entire city unless this is appropriate). These estimates are designed to represent average subsidence values across the whole subsiding area within each city. Supplementary Table 2 summarises the coastal cities considered and the subsidence values used.

410

415

Socio-economic Scenarios

Population exposure is obtained by overlaying Shuttle Radar Topography Mission (SRTM) elevation data^{50,51} with Global Rural-Urban Mapping Project (GRUMP) population data⁵², using resampling methods³⁹. As coastal urbanization trends play a major role in the population exposure analysis in this study, we use five regionalized population growth projections³⁹ based on the Shared Socio-economic Pathways (SSP2)^{23,53-55}. As the population projections do not differ much until the middle of the 21st century, we only report the one based on the middle-of-the-road scenario from the Shared Socio-economic Pathways (SSP2) in the main paper. Results for other population projections are shown in the Extended Data. We note that other population datasets would lead to different quantitative outputs as demonstrated in the analysis of Hinkel et al³¹. However, the main results in the article based on population weighting are unlikely to be sensitive to these differences as the relative distribution of population along the coast is common to all global population datasets.

420

425

430 In terms of population statistics, we consider the population living below the 10 m contour in
2015 for the population weighting of sea-level rise comprising 768 million people. To estimate
population exposure to coastal flooding we also consider the coastal flood plain population living
below the 100-year flood elevation which is dynamic in time due to relative sea-level change and
population change. This population was 235 million people in 2015.

435

Mean and extreme sea-level rise scenarios to 2050

For SLR projections we use three global-mean SLR scenarios taken from Hinkel et al³¹: the 50th
percentile of RCP2.6, RCP4.5 and RCP8.5 using the HadGEM-ES2 model⁵⁶. Extreme water
levels are assumed to uniformly increase with SLR, following 20th century observations⁵⁷.

440 Extreme water level distributions are taken from the GTSR database⁵⁸ and referenced to GeoID
to be compatible with SRTM data⁵⁹.

Regional definitions utilised:

The 23 global coastal regions used in this study are defined by Future Earth Coast, formerly
445 Land Ocean Interactions in the Coastal Zone (LOICZ), and are similar to earlier regional
definitions^{60,61}. These 23 regions divide the world's coast into geographical subsets, as defined in
Supplementary Table 3.

Weighting Approach:

450 To compute global average values of the relative SLR components and their sums, the weighted
average (*wrslr*) is computed as:

$$wrslr = \frac{\sum_{cls}(rslr(cls)*w(cls))}{\sum_{cls} w(cls)} \quad \text{Eq.1}$$

where $rslr(cls)$ is the relative sea-level change in each coastline segment (cls).

455 For length-weighted global average we set $w(cls)$ to the length of the coastline segment (cls). For population-weighted global average we set $w(cls)$ to the population living in the Low Elevation Coastal Zone (i.e., the population living within 10-m elevation of mean sea level⁶²) in each segment in 2015. In this analysis, the global coastal length totals 691,017 km and the global LECZ population is 768 million in 2015.

460

Coastal Flood Plain Population:

For the population in the flood plain we consider the 100-year flood plain (using water levels from Muis et al⁵⁸) based on the elevation data from the SRTM and the population scenarios mentioned above. Changes with time are evaluated per segment assuming SLR (as defined above), *subsidence* (or uplift) as defined above and population change (as defined above).

465

Coastal adaptation including coastal defences are not considered, and the results simply reflect the flood plain population.

Studies before Muis et al⁵⁹ did not consider the difference in vertical datum of extreme sea levels and global land elevation and thus underestimated population exposure to flooding. While extreme water level datasets such as GTSR⁵⁹ use mean sea level as vertical datum, global elevation datasets, such as SRTM, are referenced to the EGM96 geoid⁶³. The offset between mean sea level and the geoid can be up to 1.5 m, due to the dynamic sea surface of the ocean⁶⁴

470

and largely determined by ocean currents. Correcting the vertical datum increases the population
475 exposed to the 100-year flood event by 39-60%⁵⁹.

As noted earlier, other population scenarios would lead to different quantitative estimates of
coastal flood plain population (see Hinkel et al³¹), but the relative distribution of population
480 along the coast would be similar. Hence, it would have little influence on the weighting by
population described above.

Acknowledgments:

We thank Jason Ericson for sharing his dataset on delta subsidence.

Funding:

RJN was supported under the Deltas, vulnerability and Climate Change: Migration and
Adaptation (DECCMA) project (IDRC 107642) under the Collaborative Adaptation Research
Initiative in Africa and Asia (CARIAA) programme with financial support from the U.K.
Government's Department for international Development (DFID) and the International
490 Development Research Centre (IDRC), Canada and the PROTECT Project. The views expressed
in this work are those of the creators and do not necessarily represent those of DFID and IDRC
or their boards of governors. We thank the ESA CCI sea level project for providing the data and
CNES for providing the data from Topex, Jason 1 2 and 3. Other portions of this research were
made possible by support from the European Union through the projects RISES-AM (funded by
495 the European Commission's Seventh Framework Programme, 2007 – 2013, under the grant

agreement number 603396), GREEN-WIN and COACCH (funded by European Union's Horizon 2020 research and innovation programme under grant agreement No 642018 and No 776479, respectively). Further funding was received through to projects INSeaPTION and ISIPedia which are part of ERA4CS, an ERA-NET initiated by JPI Climate, and funded by FORMAS (SE), BMBF (DE, grant No 01LS1711C and No 01LS1703A), BMWF (AT), IFD (DK), MINECO (ES), ANR (FR) with co-funding by the European Union (Grant 690462). This publication was supported by PROTECT. This project has received funding from the European Union's Horizon 2020 research and innovation programme under grant agreement No 869304, PROTECT contribution number 8.

500

505

Author contributions:

RJN, DL and JH designed and conducted the analysis and wrote the main paper. They also prepared the city subsidence and GIA data. SB and SH contributed to city subsidence data and prepared the data on delta subsidence. AT and JM prepared the socio-economic data. BM provided the satellite sea-level data and the expertise on climate-induced coastal sea-level rise. JF contributed to the city subsidence data from Asia, especially China. All authors read paper drafts and approved the final version.

510

Competing interests: "Authors declare no competing interests."

515

Data Availability Statement:

All datasets used in the production of this paper are available from <http://doi.org/10.5281/zenodo.4434773>. The sea-level data is referenced under the following

DOI: [10.5270/esa-sea_level_cci-1993_2015-v_2.0-201612](https://doi.org/10.5270/esa-sea_level_cci-1993_2015-v_2.0-201612) . It is freely available from

<http://www.esa-sealevel-cci.org/products>

520

Computer Code Availability Statement:

The R code used to produce the numbers, tables and figures is available from

<http://doi.org/10.5281/zenodo.4434773>

525

Correspondence and requests for materials should be addressed to Robert Nicholls

Robert.nicholls@uea.ac.uk

References:

530

30 Hinkel, J. *et al.* A global analysis of erosion of sandy beaches and sea-level rise: An application of DIVA. *Global and Planetary Change* **111**, 150-158, <https://doi.org/10.1016/j.gloplacha.2013.09.002> (2013).

31 Hinkel, J. *et al.* Coastal flood damage and adaptation costs under 21st century sea-level rise. *Proceedings of the National Academy of Sciences* **111**, 3292, <https://doi.org/10.1073/pnas.1222469111> (2014).

535

32 Schuerch, M. *et al.* Future response of global coastal wetlands to sea-level rise. *Nature* **561**, 231-234, <https://doi.org/10.1038/s41586-018-0476-5> (2018).

33 Vafeidis, A. T. *et al.* A new global coastal database for impact and vulnerability analysis to sea-level rise. *Journal of Coastal Research* **24**, 917-924, (2008).

540

34 Nicholls, R. J. *et al.* Ranking port cities with high exposure and vulnerability to climate extremes - Exposure estimates. (OECD Publishing, Paris, France, 2008) <https://doi.org/10.1787/011766488208>

35 National Research Council. *Sea-level rise for the coasts of California, Oregon, and Washington: Past, present, and future.* (National Academic Press, 2012).

545

36 Ostanciaux, E., Husson, L., Choblet, G., Robin, C. & Pedoja, K. Present-day trends of vertical ground motion along the coast lines. *Earth-Science Reviews* **110**, 75-92, <https://doi.org/10.1016/j.earscirev.2011.10.004> (2012).

37 Pfeffer, J. & Allemand, P. The key role of vertical land motions in coastal sea level variations: A global synthesis of multisatellite altimetry, tide gauge data and GPS measurements. *Earth and Planetary Science Letters* **439**, 39-47, <https://doi.org/10.1016/j.epsl.2016.01.027> (2016).

550

- 38 Phien-wej, N., Giao, P. H. & Nutalaya, P. Land subsidence in Bangkok, Thailand. *Engineering Geology* **82**, 187-201, <https://doi.org/10.1016/j.enggeo.2005.10.004> (2006).
- 39 Merkens, J.-L., Lincke, D., Hinkel, J., Brown, S. & Vafeidis, A. T. Regionalisation of
555 population growth projections in coastal exposure analysis. *Climatic Change* **151**, 413-
426, <https://doi.org/10.1007/s10584-018-2334-8> (2018).
- 40 The Climate Change Initiative Coastal Sea Level Team *et al.* Coastal sea level anomalies
and associated trends from Jason satellite altimetry over 2002–2018. *Scientific Data* **7**,
<https://doi.org/10.1038/s41597-020-00694-w> (2020).
- 41 Wöppelmann, G. & Marcos, M. Vertical land motion as a key to understanding sea level
560 change and variability. *Reviews of Geophysics* **54**, 64-92,
<https://doi.org/10.1002/2015RG000502> (2016).
- 42 Brown, S. & Nicholls, R. J. Subsidence and human influences in mega deltas: The case of
the Ganges–Brahmaputra–Meghna. *Science of The Total Environment* **527-528**, 362-374,
<https://doi.org/10.1016/j.scitotenv.2015.04.124> (2015).
- 565 43 Erban, L. E., Gorelick, S. M. & Zebker, H. A. Groundwater extraction, land subsidence,
and sea-level rise in the Mekong Delta, Vietnam. *Environmental Research Letters* **9**,
084010, <https://doi.org/10.1088/1748-9326/9/8/084010> (2014).
- 44 Minderhoud, P. S. J. *et al.* Impacts of 25 years of groundwater extraction on subsidence
in the Mekong delta, Vietnam. *Environmental Research Letters* **12**, 064006,
570 <https://doi.org/10.1088/1748-9326/aa7146> (2017).
- 45 Tos, L., Da Lio, C., Strozzi, T. & Teatini, P. Combining L- and X-Band SAR
interferometry to assess ground displacements in heterogeneous coastal environments:
The Po River Delta and Venice Lagoon, Italy. *Remote sensing* **8**, 308,
<https://doi.org/10.3390/rs8040308> (2016).
- 575 46 Wang, H. *et al.* InSAR reveals coastal subsidence in the Pearl River Delta, China.
Geophysical Journal International **191**, 1119-1128,
<https://doi.org/https://doi.org/10.1111/j.1365-246X.2012.05687.x> (2012).
- 47 Meckel, T. A., Ten Brink, U. S. & Williams, S. J. Sediment compaction rates and
subsidence in deltaic plains: numerical constraints and stratigraphic influences. *Basin*
580 *Research* **19**, 19-31, <https://doi.org/10.1111/j.1365-2117.2006.00310.x> (2007).
- 48 Hallegatte, S., Green, C., Nicholls, R. J. & Corfee-Morlot, J. Future flood losses in major
coastal cities. *Nature Climate Change* **3**, 802-806, <https://doi.org/10.1038/nclimate1979>
(2013).
- 585 49 Chaussard, E., Amelung, F., Abidin, H. & Hong, S.-H. Sinking cities in Indonesia: ALOS
PALSAR detects rapid subsidence due to groundwater and gas extraction. *Remote*
Sensing of Environment **128**, 150-161, <https://doi.org/10.1016/j.rse.2012.10.015> (2013).
- 50 Rabus, B., Eineder, M., Roth, A. & Bamler, R. The shuttle radar topography mission—a
new class of digital elevation models acquired by spaceborne radar. *ISPRS Journal of*
Photogrammetry and Remote Sensing **57**, 241-262, [https://doi.org/10.1016/S0924-
2716\(02\)00124-7](https://doi.org/10.1016/S0924-2716(02)00124-7) (2003).
- 590 51 Jarvis, A., Reuter, H. I., Nelson, A. & Guevara, E. Hole-filled SRTM for the globe
Version 4. (2008) <http://srtm.csi.cgiar.org>.
- 52 Center for International Earth Science Information Network - CIESIN - Columbia
University, International Food Policy Research Institute - IFPRI, The World Bank &
595 Centro Internacional de Agricultura Tropical - CIAT. *Global Rural-Urban Mapping*

Project, Version 1 (GRUMPv1): Population Count Grid. (NASA Socioeconomic Data and Applications Center (SEDAC), 2011). <https://doi.org/10.7927/H4VT1Q1H>.

53 IIASA. SSP Database. (2012) <https://tntcat.iiasa.ac.at/SspDb>.

54 O'Neill, B. C. *et al.* A new scenario framework for climate change research: the concept
600 of shared socioeconomic pathways. *Climatic Change* **122**, 387-400,
<https://doi.org/10.1007/s10584-013-0905-2> (2014).

55 Samir, K. C. & Lutz, W. The human core of the shared socioeconomic pathways:
Population scenarios by age, sex and level of education for all countries to 2100. *Global
605 Environmental Change* **42**, 181-192, <https://doi.org/10.1016/j.gloenvcha.2014.06.004>
(2017).

56 Collins, W. J. *et al.* Development and evaluation of an Earth-System model – HadGEM2.
Geoscientific Model Development **4**, 1051-1075, [https://doi.org/10.5194/gmd-4-1051-
2011](https://doi.org/10.5194/gmd-4-1051-2011) (2011).

57 Menéndez, M. & Woodworth, P. L. Changes in extreme high water levels based on a
610 quasi-global tide-gauge data set. *Journal of Geophysical Research: Oceans* **115**,
<https://doi.org/10.1029/2009JC005997> (2010).

58 Muis, S., Verlaan, M., Winsemius, H. C., Aerts, J. C. J. H. & Ward, P. J. A global
reanalysis of storm surges and extreme sea levels. *Nature Communications* **7**, 11969,
<https://doi.org/10.1038/ncomms11969> (2016).

615 59 Muis, S. *et al.* A comparison of two global datasets of extreme sea levels and resulting
flood exposure. *Earth's Future* **5**, 379-392, <https://doi.org/10.1002/2016EF000430>
(2017).

60 Hoozemans, F. M. J., Marchand, M. & Pennekamp, H. A. Sea level rise: A global
vulnerability analysis: Vulnerability assessment for population, coastal wetlands and rice
620 production on a global scale. (Delft Hydraulics, the Netherlands, 1993)
[https://repository.tudelft.nl/islandora/object/uuid:651e894a-9ac6-49bf-b4ca-
9aedef51546f](https://repository.tudelft.nl/islandora/object/uuid:651e894a-9ac6-49bf-b4ca-9aedef51546f).

61 Nicholls, R. J. & Hoozemans, F. M. J. in *Encyclopedia of Coastal Science* (ed Maurice
L. Schwartz) Ch. Global vulnerability analysis, 486-491 (Springer Netherlands, 2005)
625 https://doi.org/10.1007/1-4020-3880-1_155

62 McGranahan, G., Balk, D. & Anderson, B. The rising tide: assessing the risks of climate
change and human settlements in low elevation coastal zones. *Environment and
Urbanization* **19**, 17-37, <https://doi.org/10.1177/0956247807076960> (2007).

63 Farr, T. G. *et al.* The Shuttle Radar Topography Mission. *Reviews of Geophysics* **45**,
630 <https://doi.org/https://doi.org/10.1029/2005RG000183> (2007).

64 Schaeffer, M., Hare, W., Rahmstorf, S. & Vermeer, M. Long-term sea-level rise implied
by 1.5 °C and 2 °C warming levels. *Nature Climate Change* **2**, 867-870,
<https://doi.org/10.1038/nclimate1584> (2012).

65 Becker, M. *et al.* Water level changes, subsidence, and sea level rise in the Ganges–
Brahmaputra–Meghna delta. *Proceedings of the National Academy of Sciences* **117**,
635 1867, <https://doi.org/10.1073/pnas.1912921117> (2020).

66 Higgins, S. A. *Measurements of deltas at risk* (University of Colorado, Boulder,
Colorado, USA, 2014).

- 67 Wöppelmann, G. *et al.* Is land subsidence increasing the exposure to sea level rise in
640 Alexandria, Egypt? *Geophysical Research Letters* **40**, 2953-2957,
<https://doi.org/10.1002/grl.50568> (2013).
- 68 Gebremichael, E. *et al.* Assessing land deformation and sea encroachment in the Nile
Delta: A radar interferometric and inundation modeling approach. *Journal of*
645 *Geophysical Research: Solid Earth* **123**, 3208-3224,
<https://doi.org/10.1002/2017JB015084> (2018).
- 69 Deltacommissie. Working together with water. A living land builds for its future. (2008)
<http://www.deltacommissie.com/en/advies>.
- 70 Suanez, S. & Provansal, M. Morphosedimentary behaviour of the deltaic fringe in
comparison to the relative sea-level rise on the Rhone delta. *Quaternary Science Reviews*
650 **15**, 811-818, [https://doi.org/10.1016/S0277-3791\(96\)00067-4](https://doi.org/10.1016/S0277-3791(96)00067-4) (1996).
- 71 Samsonov, S. V. *et al.* Rapidly accelerating subsidence in the Greater Vancouver region
from two decades of ERS-ENVISAT-RADARSAT-2 DInSAR measurements. *Remote*
Sensing of Environment **143**, 180-191, <https://doi.org/10.1016/j.rse.2013.12.017> (2014).
- 72 Mazzotti, S., Lambert, A., Van der Kooij, M. & Mainville, A. Impact of anthropogenic
655 subsidence on relative sea-level rise in the Fraser River delta. *Geology* **37**, 771-774,
<https://doi.org/10.1130/g25640a.1> (2009).
- 73 Zhao, J. K., Wu, M. J., Liu, S. X. & Shen, H. Z. The relation between groundwater
exploitation and land subsidence in the coast plain of Zhejiang Province (in Chinese).
Geological Journal of China Universities **12**, 185-194, (2006).
- 660 74 Xu, N. Z., Jiang, Y. H., Wang, J. D., Liu, H. & Jia, J. The types and characteristics of the
ground subsidence in southeastern China coastal region (in Chinese). *Journal of*
Catastrophology **20**, 67-72, (2005).
- 75 Xue, Y.-Q., Zhang, Y., Ye, S.-J., Wu, J.-C. & Li, Q.-F. Land subsidence in China.
Environmental Geology **48**, 713-720, <https://doi.org/10.1007/s00254-005-0010-6> (2005).
- 665 76 Yang, C., Pan, L. Y. & Yu, C. Land subsidence control in Wenzhou, Zhejiang (in
Chinese). *Low Temperature Architecture Technology* **158**, 114-115, (2011).
- 77 Orejarena-Rondón, A. F. *et al.* Coastal impacts driven by sea-level rise in Cartagena de
Indias. *Frontiers in Marine Science* **6**, <https://doi.org/10.3389/fmars.2019.00614> (2019).
- 78 Chatterjee, R. S. *et al.* Subsidence of Kolkata (Calcutta) City, India during the 1990s as
670 observed from space by Differential Synthetic Aperture Radar Interferometry (D-InSAR)
technique. *Remote Sensing of Environment* **102**, 176-185,
<https://doi.org/10.1016/j.rse.2006.02.006> (2006).
- 79 Sahu, P. & Sikdar, P. K. Threat of land subsidence in and around Kolkata City and East
Kolkata Wetlands, West Bengal, India. *Journal of Earth System Science* **120**, 435-446,
675 <https://doi.org/10.1007/s12040-011-0077-2> (2011).
- 80 Abidin, H. Z., Andreas, H., Gumilar, I., Sidiq, T. P. & Fukuda, Y. Land subsidence in
coastal city of Semarang (Indonesia): characteristics, impacts and causes. *Geomatics,*
Natural Hazards and Risk **4**, 226-240, <https://doi.org/10.1080/19475705.2012.692336>
(2013).
- 680 81 Deltares. *Sinking cities: An integrated approach towards solutions*. (Deltares, 2014).
- 82 Kasmarek, M. C., Gabrysch, R. K. & Johnson, M. R. Estimated land-surface subsidence
in Harris County, Texas, 1915-17 to 2001. Report No. 3097, (Reston, VA, 2009)
<http://pubs.er.usgs.gov/publication/sim3097>. <https://doi.org/10.3133/sim3097>

- 685 83 Dixon, T. H. *et al.* Subsidence and flooding in New Orleans. *Nature* **441**, 587-588,
<https://doi.org/10.1038/441587a> (2006).
- 84 84 Nguyen, Q. T. The main causes of land subsidence in Ho Chi Minh City. *Procedia*
Engineering **142**, 334-341, <https://doi.org/10.1016/j.proeng.2016.02.058> (2016).
- 85 85 Nicholls, R. J. *et al.* A global analysis of subsidence, relative sea-level change and coastal
690 flood exposure. Dataset. <http://doi.org/10.5281/zenodo.4434773> (2021).

List of Tables

695 **Table 1:** Contribution of the climate and geological components to relative sea-level change for length-weighted and population-weighted cases, respectively. Average values are reported, except for cities and the global-mean sum where a low/high range is used to express the uncertainty in subsidence (see Supplementary Table 2).

List of Figures

700 **Fig 1:** Cumulative distribution of contemporary length-weighted and population-weighted coastal relative sea-level rise, respectively. This includes lower and upper estimates to express uncertainty, although for length weighting the difference is too small to be seen.

705 **Fig 2:** Average relative sea-level rise for 23 coastal world regions. (a) Length-weighted and (b) population-weighted. (see Supplementary Table 3 for region definitions).

710 **Fig 3:** Global population in the coastal flood plain from 2015 to 2050. This considers sea-level rise scenarios under RCP2.6, RCP4.5 and RCP8.5 emissions, as well as no climate-induced sea-level rise as a reference, and assumes the SSP2 socio-economic scenario. Subsidence/GIA assumptions as indicated. (a) No vertical land movement. (b) GIA only. (c) GIA and delta subsidence. (d) GIA, delta and uncontrolled city subsidence. (e) GIA, delta and city subsidence controlled to 5 mm/yr. The uncertainty bands reflect uncertainty in rates of city subsidence (see Fig. 1). Simulations start in 1995, while the flood plain is defined based on the 100-year event.

715

List of Extended Data Figures

720

Extended Data Fig 1: Cumulative distribution of contemporary coastal relative SLR. (a) length-weighted, (b) population-weighted. Each panel shows climate-induced SLR alone, and then progressively adds the other components comprising: (1) GIA, (2) GIA and delta subsidence combined, and (3) GIA, delta subsidence and uncontrolled city subsidence combined. For uncontrolled city subsidence, the uncertainty is considered by using a low and high estimate. For length weighting, the main change occurs due to adding the GIA component, which reduces the median and mean SLR. Considering delta and city subsidence has little effect as only 6.5 percent and 0.8 percent of the world's coast length are affected. For population weightings, adding GIA also has an effect, but it is smaller than for length weighting being -0.3 mm/yr on mean SLR. This reflects that the coastal population is preferentially located in areas where GIA causes subsidence, which counters the effect GIA has when considering length weighting. Adding delta and then uncontrolled city subsidence has a significant effect reflecting the large populations in these areas. In the median, these two components add 1.19 mm/yr and an additional 0.62 mm/yr of SLR rise, respectively. The asymmetric distribution of the high-end tail leads to a larger effect on the mean SLR at 1.6 mm/yr due to delta subsidence alone, and an additional 2.7 to 4.8 mm/yr due to city subsidence alone (Table 1).

725

730

735

Extended Data Fig 2: Sea-level rise components versus coastal population density for all the coastal segments considered in the analysis. These comprise (a) climate-induced sea-level rise only, (b) GIA only, (c) high estimates of uncontrolled city subsidence only, (d) delta subsidence only, and (e) the sum of all four components considered previously. The linear best fit and the

explained variance are shown in each case. While the explained variance with such a linear fit is small, the slopes are significantly different from zero in all cases.

740 **Extended Data Fig 3:** Global total of people living in the coastal flood plain from 2015 to 2050
under a range of socio-economic and climate scenarios. These comprise five different SSP-based
regionalised population scenarios (SSP1 to SSP5), and no climate-induced SLR and the RCP2.6
and RCP8.5 SLR scenarios, respectively. Assumptions concerning geological components of
relative SLR are as follows: Column (a) No geological component, Column (b) GIA only,
745 Column (c) GIA and delta subsidence, Column (d) GIA, delta and uncontrolled city subsidence.
Column (e) GIA, delta and controlled city subsidence (to a maximum of 5 mm/yr). The
uncertainty bands in (d) reflect uncertainty in the rates of city subsidence (see Fig 1). All
simulations start in 1995. The results indicate little variation between SSPs to 2050.

750 **List of Supplementary Tables**

Supplementary Table 1: Subsidence rates applied by delta: a positive value indicates
subsidence and a negative value indicated aggradation. Expert judgement draws on Meckel et
al⁴⁷.

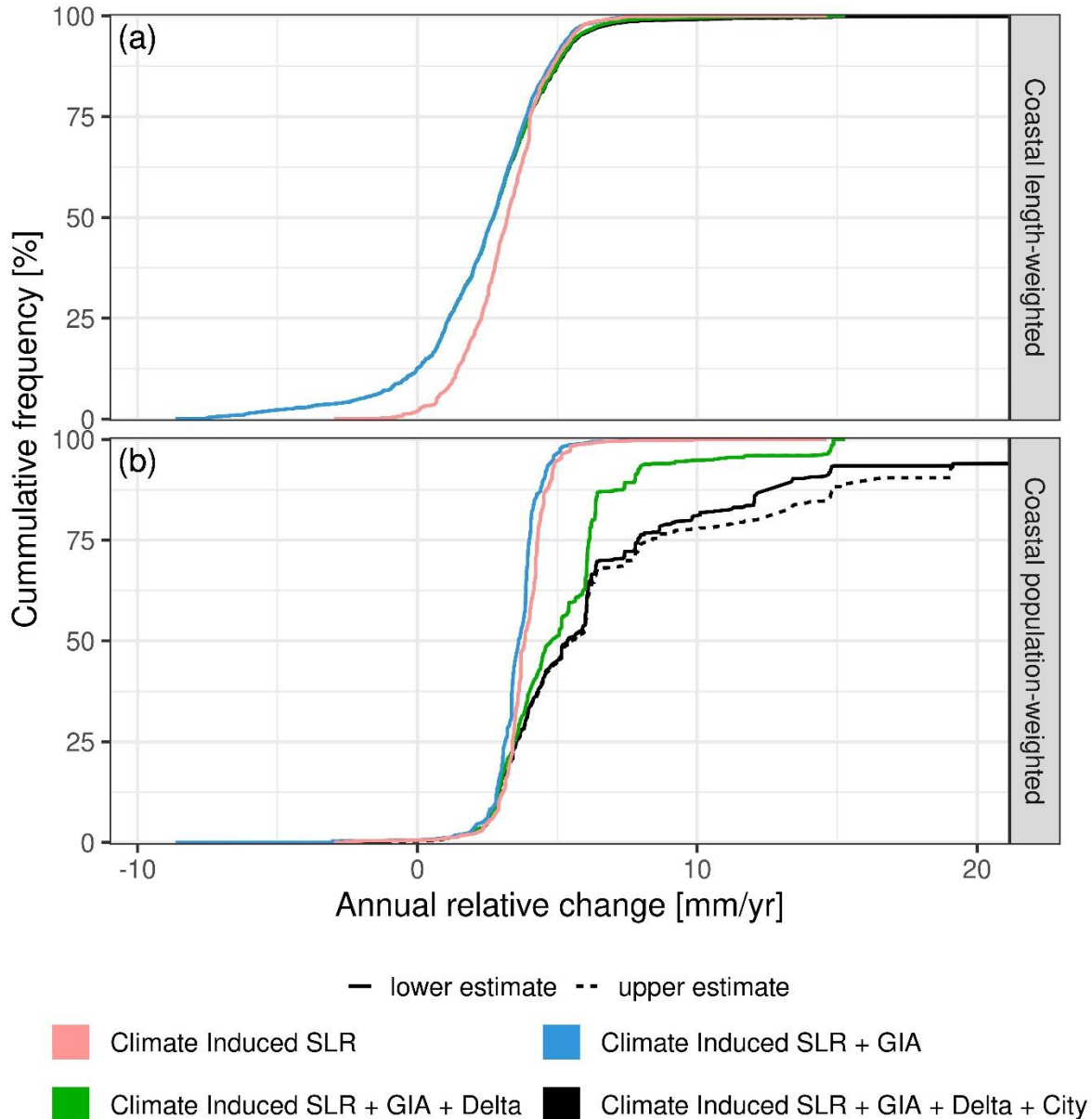
Supplementary Table 2: Additional subsidence rates applied by city: a positive value indicates
755 subsidence. If cities are not listed here, no additional subsidence is applied.

Supplementary Table 3: Regional definitions as used in Fig 2.

Supplementary Table 4: Regional-mean relative sea-level rise comparing length and population
weightings. Rows coloured yellow see a 50 to 100% increase, while rows coloured green see

more than 100% increase moving from length to population weightings, respectively. In the
760 other rows, changes are within +50%.

Extended Data Figures

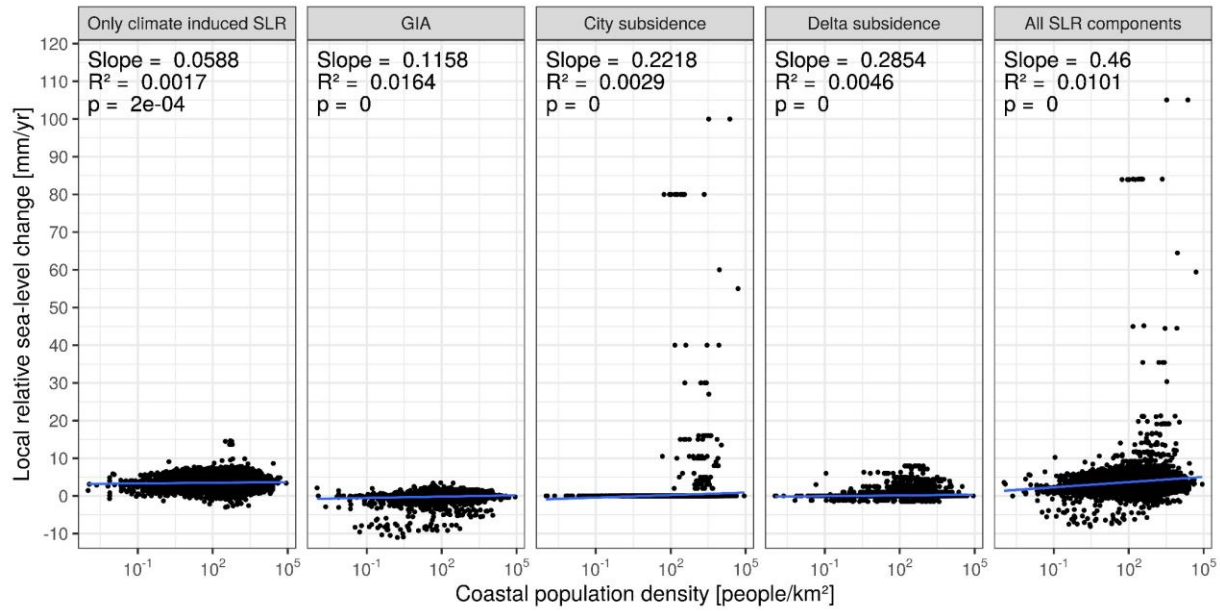


765 **Extended Data Fig 1:** Cumulative distribution of contemporary coastal relative SLR. (a) length-weighted, (b) population-weighted. Each panel shows climate-induced SLR alone, and then progressively adds the other components comprising: (1) GIA, (2) GIA and delta subsidence combined, and (3) GIA, delta subsidence and uncontrolled city subsidence combined. For uncontrolled city subsidence, the uncertainty is considered by using a low and high estimate.

770 For length weighting, the main change occurs due to adding the GIA component, which reduces the median and mean SLR. Considering delta and city subsidence has little effect as only 6.5 percent and 0.8 percent of the world's coast length are affected. For population weightings, adding GIA also has an effect, but it is

775

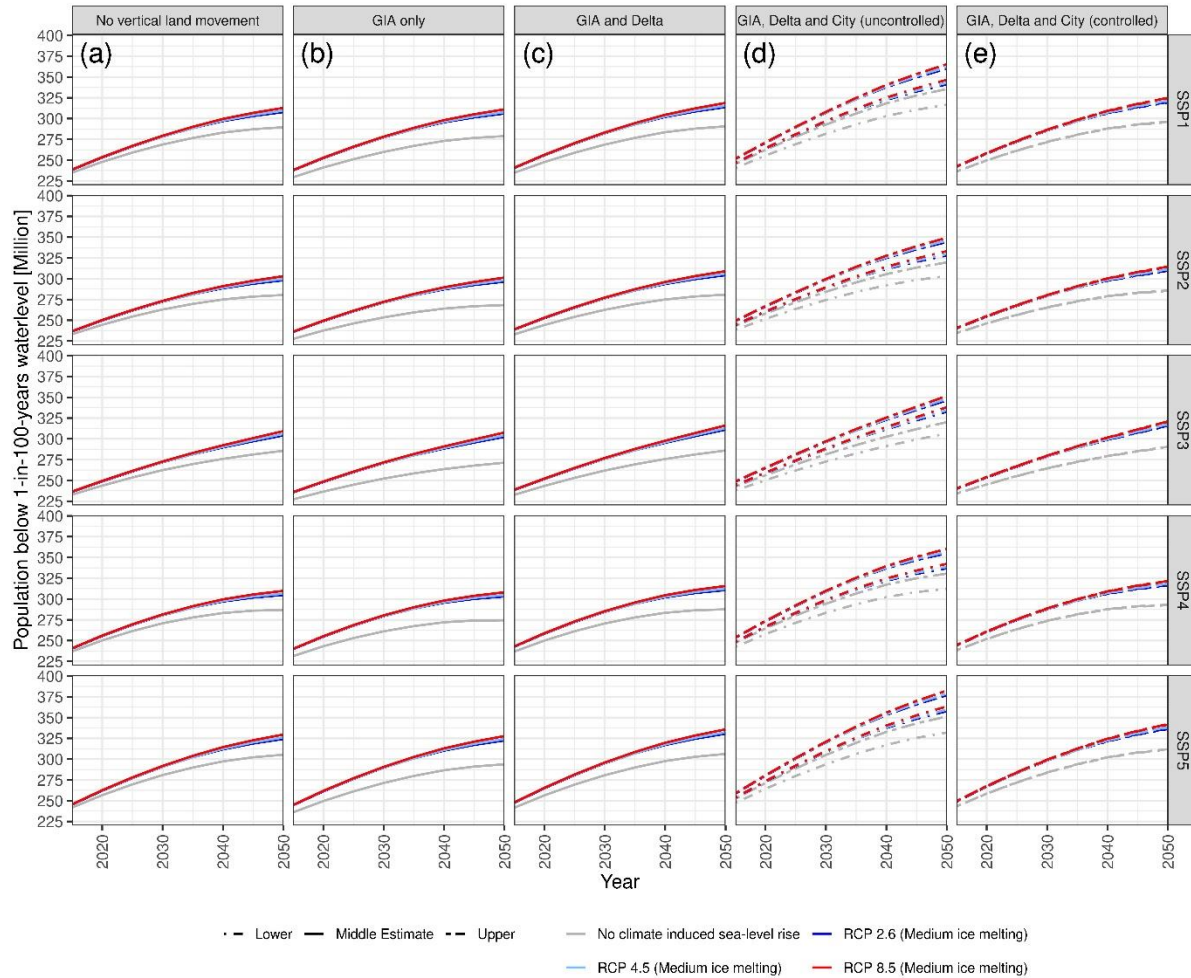
smaller than for length weighting being -0.3 mm/yr on mean SLR. This reflects that the coastal population is preferentially located in areas where GIA causes subsidence, which counters the effect GIA has when considering length weighting. Adding delta and then uncontrolled city subsidence has a significant effect reflecting the large populations in these areas. In the median, these two components add 1.19 mm/yr and an additional 0.62 mm/yr of SLR rise, respectively. The asymmetric distribution of the high-end tail leads to a larger effect on the mean SLR at 1.6 mm/yr due to delta subsidence alone, and an additional 2.7 to 4.8 mm/yr due to city subsidence alone (Table 1).



780

Extended Data Fig 2: Sea-level rise components versus coastal population density for all the coastal segments considered in the analysis. These comprise (a) climate-induced sea-level rise only, (b) GIA only, (c) high estimates of uncontrolled city subsidence only, (d) delta subsidence only, and (e) the sum of all four components considered previously. The linear best fit and the explained variance are shown in each case. While the explained variance with such a linear fit is small, the slopes are significantly different from zero in all cases.

785



790 **Extended Data Fig 3:** Global total of people living in the coastal flood plain from 2015 to 2050
 795 under a range of socio-economic and climate scenarios. These comprise five different SSP-based regionalised population scenarios (SSP1 to SSP5), and no climate-induced SLR and the RCP2.6 and RCP8.5 SLR scenarios, respectively. Assumptions concerning geological components of relative SLR are as follows: Column (a) No geological component, Column (b) GIA only, Column (c) GIA and delta subsidence, Column (d) GIA, delta and uncontrolled city subsidence. Column (e) GIA, delta and controlled city subsidence (to a maximum of 5 mm/yr). The uncertainty bands in (d) reflect uncertainty in the rates of city subsidence (see Fig 1). All simulations start in 1995. The results indicate little variation between SSPs to 2050.